Subpixel Registration Using a Concentric Ring Fiducial

Lawrence O'Gorman
Alfred M. Bruckstein
Chinmoy B. Bose
Israel Amir

AT&T Bell Laboratories
Murray Hill, New Jersey 07974

ABSTRACT

One way to perform registration and alignment for machine assembly is with respect to precisely located landmarks, called fiducials, that are located by machine vision means. For applications such as electronics assembly, where densities are high and tolerances must be low, the precision by which the fiducials are located affects everything aligned relative to them. We examine the effects of spatial sampling and image noise on the precision by which the centroids of different geometric shapes can be determined. The concentric ring fiducial — a bull's-eye pattern — is identified as having desirable qualities of high location precision and rotational invariance. The performance of the concentric fiducial, as a function of diameter, number of rings, and ring spacing, has been tested, and these results are shown.

1. Introduction

Electronics assembly, robotics manipulation, and many other manufacturing applications, require precise registration to assure proper positioning and alignment. One way to perform registration is to position everything with respect to one or more landmarks, called *fiducial marks*, or simply *fiducials*. For the electronics application, fiducials are positioned in precise and known locations relative to circuit traces. Then registration is performed relative only to the fiducials, independent of any imprecision of absolute positioning on the machine. The number of fiducials required depends on the degrees of freedom of the object position and shape, however the precision is only as good as that of each fiducial. In this paper, we deal with the location of a single fiducial by machine vision means. Subpixel precision in determining the fiducial location is examined as a function of its shape and size, and imaging factors including sampling resolution and noise. This paper extends past work [1], whose results have since proven effective in a production environment.

There is no doubt that registration is important, but why is it important that it be to subpixel precision? The answer to this addresses the classic engineering tradeoff between efficiency and effectiveness. On one hand, there is the requirement that registration be performed at or above a specified precision. However, the use of too high a resolution will add to the computation time with no additional benefit. Even for a conservative design where "over-engineering" is accepted, an idea of the approximate bounds of this safety region is helpful. Knowledge of the precision attainable from a specific shape and size will enable both the required precision to be met, and this to be done in as efficient an implementation as possible. Therefore the benefits of methods that achieve subpixel precision can be seen from two perspectives: either as a means to obtain higher precision, or as a means to obtain the same precision at less computational cost.

The focus in this paper is the precision attainable via the centroid measurement. This centroid measurement is determined from the image of the fiducial, by calculating the average of its x,y pixel coordinates. Precision is measured relative to the true (unsampled) fiducial center, and the error is the Euclidean distance between the measured centroid and the true center. (Further use of the term "centroid" without other description refers to the measured, or sampled, centroid.) The use of the centroid for location and registration is widespread in practice. It is straightforward to implement and provides subpixel precision. The centroid can be determined quickly just by accumulating three sums over the image, and this can be done in raster-scan order, so there is no need to store the image. Furthermore, there is no dependence on image resolution, nor need for any parameters to set.

Other methods, besides centroid measurement, are used for registration as well. Instead of finding the centroid, the autocorrelation peak can be used as a good measure of location [2,3]. In the latter reference, a random dot pattern is used as the fiducial because it is shown to have a high tolerance to noise. The method entails low-pass filtering of the pattern, autocorrelation, then peak searching. There are also methods for matching shapes whose boundaries are made of line segments and circular arcs [4] and the accuracy of these is discussed in [5].

Subpixel precision has also been dealt with in the literature as a problem independent of the registration application. In [6], a statistical analysis is given of spatial sampling error for straight-edged geometric shapes and the circular disk. In contrast to that paper's measurement of average and variance of the error, we place emphasis on *worst-case* error, which is more pertinent to the registration application. Analysis is given in [7], of error for straight edges, but this does not cover the circular edges of interest here. In [8,9,10], error was examined in terms of *domain* or *locale*, that is the subpixel area within which the center of the shape can move without causing a change to its sampled image. For larger, non-rectangular shapes containing many pixels, these locales become quite complicated. In [10], a bound on the precision error was found analytically for a one-dimensional line, and compared to experimental results. This is similar to the worst-case error problem in this paper, except our interest is in two-dimensional shapes. Sampling error for circular disks is analyzed in [11,12]; however neither of these papers completely addresses our problem. In the former, an iterative method is described for determining the center of the noiseless circle. In the latter, there is the limitation that the analysis is restricted to a circular disk centered exactly on a sample point.

2. Shape and Size of Simple Geometric Fiducials

In an earlier work [1] the subpixel registration precision of simple geometrically shaped fiducials was studied. Using analysis and experiment, the maximum error in the centroid due to spatial sampling was examined for different shapes and parameters. For completeness, we summarize this work here.

For purposes of analysis and experiment, the image is assumed to be binary. The binary images are created by assigning a 1 to a pixel $p(x,y)$ if its center is found to be within the analog fiducial region, and 0 otherwise. For determination of the effects of sampling, the center of the concentric fiducial was shifted uniformly within (0,0) to (0.5,0.5) at increments of 0.01 pixels in x and y. The maximum of the errors for all (50×50 = 2500) shifts within this region is found and recorded. To test the effects of size, a

Address correspondence to the first author at AT&T Bell Laboratories, Rm. 3D-455, Murray Hill, NJ, 07974. A.M. Bruckstein is visiting from the Technion, IIT, Israel.

CH2898-5/90/0000/0249$01.00 © 1990 IEEE

dimension of the fiducial is incremented in 0.25 pixel steps over a range of 2 to 22 pixels, and the change of error is examined.

For the square fiducial, it is shown in Figure 1 (and proven in [1]) that the maximum error of the centroid location varies between 0.5 and 0.25 pixels for the sidelengths of a square varying between an integer value of pixels to an integer plus a half pixel, respectively. Therefore, the best square size for least error has sidelengths equal to $n+1/2$ pixels, $n \in Z$. Larger or smaller sizes (outside of $\pm 1/2$) do not reduce or increase the maximum digitization error.

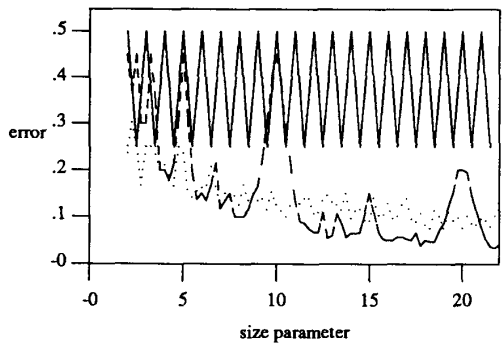

Figure 1. Maximum sampling error for the centroids of the square (solid line), diamond (dashed), and circular disk (dotted), over different lengths of sidelength, vertical diagonal, and diameter, respectively.

We choose to investigate the behavior of the diamond fiducial as a function of the ratio between the diagonals. For this, the horizontal diagonal is fixed at 10 pixels and the vertical diagonal is varied from 2 to 22 pixels. The behavior of the maximum error in the horizontal direction is dependent on the ratio of vertical to horizontal diagonals. For the ratio 1:1, and the size parameter equal to 10, the error is the same as that of the square with integer lengths. For integer ratios, 2, 3, 4, etc., it is seen here that the maximum error peaks decrease for larger ratios, and the minimum local errors between peaks also decrease as the ratio becomes larger.

For the circular fiducial, it can be seen in Figure 1 that the maximum error decreases as the radius increases, although not monotonically. The error is appreciably less than that for the square, and this difference is greater for larger size. It is less than for the peaks of the diamond, but larger than for the valleys.

Among these shapes tested, the square is clearly inferior for precise centroid location. It is possible to design the diamond such that the ratio of axis lengths ensures a local minimum in the error. However, a small rotation in the shape will cause the error to ascend from the local minimum to one of the surrounding peaks. Depending on the magnitude of the rotation, the error for the diamond can then be much greater than that for the comparably sized (i.e. fitting in the same bounding box) circular disk. In contrast, the error for the disk is rotationally independent. Because rotational independence is attractive for fiducial registration, we choose to further examine the circular shape here.

3. Circular Fiducial — Centroid Calculations

The objective is to determine the fiducial location, and for this we measure the centroid of the fiducial from the binary image plane. For this situation, the most straightforward method of centroid determination is just to find the average of the 1-pixel locations, (M_x, M_y):

$$M_x = \frac{1}{A}\sum_y\sum_x x \cdot p(x,y)\,, \quad M_y = \frac{1}{A}\sum_y\sum_x y \cdot p(x,y)\,, \qquad (1)$$

$$\text{where} \quad A = \sum_y\sum_x p(x,y)\,, \quad p(x,y) = \{0,1\}\,,$$

and where summations are made over all pixels in the image. (For the remainder of the paper, we show only the M_x calculations; those for M_y are analogous.) In a practical situation, the general location of the fiducial is known, and a camera-view or subimage can be taken that contains only the fiducial (including some of the surrounding region and noise, but no other features).

Knowledge of the fiducial size and shape can be exploited to improve the measure. Consider that it is not necessary to sum all the pixels within the fiducial; instead, with knowledge that the disk is filled (completely 1-valued), the edges can be found, and the same centroid calculated just from these edge locations. For the edges of x-runs starting at $x_o(y)$ and ending at $x_f(y)$ for rows of y, the centroid and area can be calculated:

$$\begin{aligned} M_x &= \frac{1}{A}\sum_y \sum_{x=x_o(y)}^{x_f(y)} x \cdot p(x,y) \\ &= \frac{1}{2A}\sum_y \left[x_f^2(y)+x_f(y)-x_o^2(y)+x_o(y)\right], \\ A &= \sum_y \left[x_f(y)-x_o(y)+1\right]. \end{aligned} \qquad (2)$$

The purpose of showing how the centroid can be calculated from the edges in each dimension is to illustrate that, although calculation is for the centroid of a filled disk, the internal pixels of the disk do not actually have to be inspected. Because of this, we are free to change the values within the disk edges without affecting the centroid calculation. Since the objective is a reliable centroid measure, we choose to change internal pixel values within the disk in such a way as to improve the estimate of the centroid. Adopting the philosophy that "the more fiducials, the better" (this will be justified later), we insert into the original disk, more disks, all concentric, of a sequence of uniformly increasing radii from the inner to outer disks, and of alternating 1,0 values, as in Figure 2. We determine the centroid of each disk, treating them as filled either with 1 or 0 values. Then the weighted average of these r centroids is found, and said to be the centroid of the concentric fiducial. From reference [6], where the variance is shown to decrease linearly with increasing disk diameter. we choose to weight the moments of each disk proportionally to their respective diameters, $d(i)$. Therefore, we define the centroid for the combination of disks in the concentric pattern as,

$$M_x = \frac{1}{\sum_i d(i)} \sum_i d(i) M_x(i)\,, \quad i = 1,2,\cdots,r \qquad (3)$$

where $M_x(i)$ is calculated as for M_x in equation (2).

The advantage of this concentric configuration is that more fiducials have been added but *all additional disks are contained in the area of the original disk.* When each ring of the concentric fiducial is considered as a filled disk, we refer to the total area of these disks as their *effective area*, A_E. The effective area for r disks is,

$$A_E = \sum_{i=1}^{r} A(i) = \sum_{i=1}^{r}\sum_y \left[(x_f(y)-x_o(y)+1\right]_i . \qquad (4)$$

For a fixed diameter, d, effective area increases with the number of rings. We show below, first how the effective area is increased by adding rings, then how the effective variance is reduced due to this. The improvement in effective area can be shown for the unsampled case below. For a single disk, the area is,

$$A(1) = \frac{\pi d^2}{4}. \qquad (5)$$

Within this disk, let us build a concentric pattern of r disks with increasing diameters uniformly spaced by $\Delta d = d/(2r-1)$, from the smallest, $d_1 = \Delta d$, to the largest, $d_r = (2r-1)\Delta d = d$, and in general, $d_i = (2i-1)\Delta d$. The effective area is,

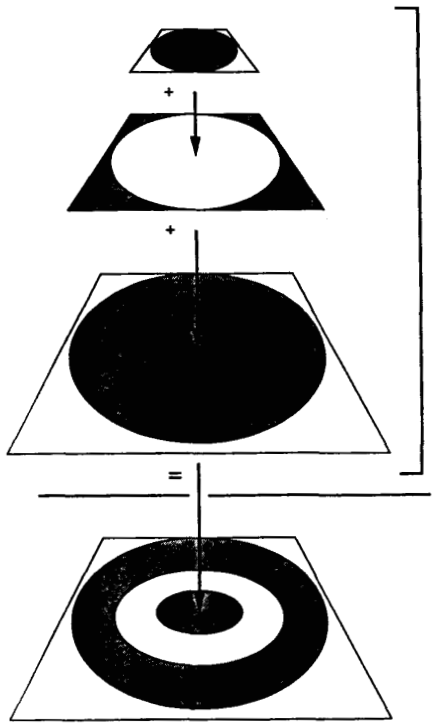

Figure 2. A fiducial with three rings can be thought of as the concentric superposition of all the disks. The area of the fiducial is that of the largest disk, but the effective area is the sum of individual disks.

$$A_E(r) = \pi\left(d_1/2\right)^2 + \pi\left(d_2/2\right)^2 + \cdots + \pi\left(d_r/2\right)^2.$$
$$= \frac{\pi d^2}{4(2r-1)^2}\sum_{i=1}^{r}(2i-1)^2 \qquad (6)$$
$$= \frac{\pi d^2 r(2r+1)}{12(2r-1)}$$

The effective area versus number of rings is plotted in Figure 3. It can be seen that for $r \geq 5$, the effective area, normalized by $A(1) = \pi d^2/4$, increases approximately as $r/3$.

Assuming the centroid measurements from each disk are independent random variables with means equal to the true centroid and variances of σ_i, it can be shown that the variance of the measured centroid from a concentric fiducial is less than that for a single disk. For a concentric fiducial of r independent disks, the effective variance is,

$$\sigma_E^2 = \sum_i \left[\frac{d(i)}{\sum_i d(i)}\right]^2 \sigma_i^2. \qquad (7)$$

It is shown by Monte Carlo simulation in [6] that the variance of the centroid estimate for a single disk is $\sigma_i^2 = k/d_i$, where k is a constant. For the outer ring whose diameter is d, the variance is $\sigma^2 = kd$. Therefore expressing the variance for each ring with respect to that for the outer,

$$\sigma_i^2 = \frac{d}{d_i}\sigma^2, \quad i = 0, \cdots, r-1.. \qquad (8)$$

Substituting this in equation (7),

$$\sigma_E^2 = \frac{\sigma^2 d}{\sum_i d(i)} \qquad (9)$$

Substituting for $d_i = (2i-1)d/(2r-1)$, and simplifying, then

$$\sigma_E^2 = \frac{2r-1}{r^2}\sigma^2. \qquad (10)$$

The effective variance, normalized by the variance for the outer disk, is plotted in Figure 3. It can be seen that the effective variance is always less than or equal to σ^2, and that it decreases for larger r with the inverse relationship approximately $2/r$.

Having shown the above development, it must be cautioned that the assumption was made of independent ring centroids. There is experimental evidence (in Section 4) that the rings are not independent, but weakly correlated. The degree of correlation affects how closely the equivalent variance in equation (10) matches the true results. In Section 4, we give test results that show how the centroid error is reduced by increasing the number of concentric rings.

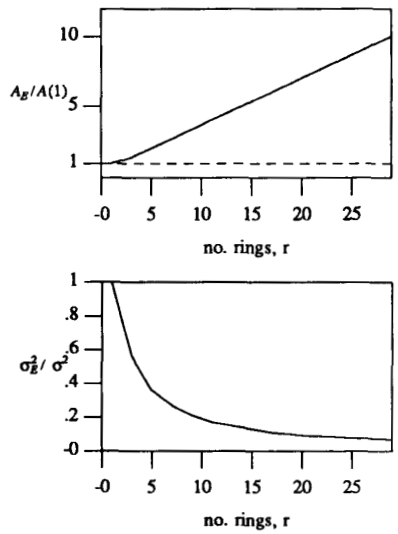

Figure 3. The top plot shows that effective area increases approximately as the number of rings times $1/3$. The bottom plot shows that the variance decreases with the number of rings.

4. Concentric Fiducial — Experimental Results

Tests were made on the performance of the concentric fiducial for subpixel translations on a sampling plane, and with noise. For these, the centroid was measured from the sampled, binary image, and the Euclidean distance between the true centroid and the measured centroid was calculated, and called the *error*. Two sets of tests were carried out. In one, a noiseless fiducial was shifted in subpixel increments on the sampling plane, and the error due to sampling determined. In the other, noise was added to the image, and the error due to this noise found.

For the determination of the effects of sampling, the center of the concentric fiducial was shifted uniformly within (0,0) to (0.5,0.5) pixels at increments of 0.01 pixels in x and y, and the maximum error was found as described in Section 2. Concentric fiducials of three outer diameters, $d_r = \{50, 100, 300\}$, and with a number of rings, $r = \{1, 3, 5, \cdots, 29\}$, were tested.

The results are plotted in Figure 4. Note first that, as the number of rings is increased, the maximum error generally decreases. Also, for larger diameters, the error peaks are generally lower. However, also note that the plots are not smooth. We will discuss these apparent anomalies as well as the general trends in Section 5.

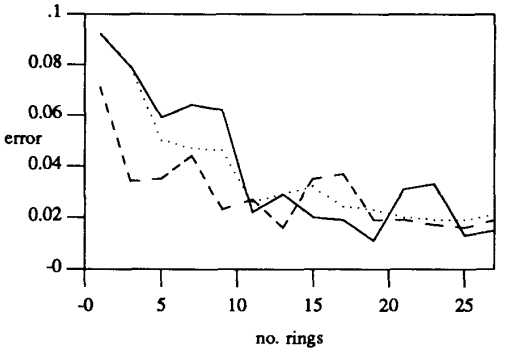

Figure 4. Maximum sampling error for concentric fiducial. Solid line is for outer ring size of 50, dashed for 100, and dotted for 300.

For the second set of tests, the fiducial was centered at (0,0), and noise introduced with the following characteristics. At each pixel location, noise was added with probability P of setting the value to 1 or 0. This yields a random spatial distribution of 1-valued noise outside the fiducial area, and 0-valued noise within the fiducial area. Noise probabilities of $P = 0.05$ and $P = 0.1$ were tested here. After the noise is added, a simple morphological filter was applied to reduce isolated 1 or 0 noise, and to smooth spurs and indentations on boundaries. Thus, the addition and reduction of noise leaves rings with noisy boundaries. For each test case, 15 images were taken with different random noise. The results show the average and the standard deviation of the maximum errors over the 15 sample images of each case.

The results are plotted in Figures 5 and 6. They indicate that: i) both the error and standard deviation generally decrease when the number of rings increases; ii) error is generally smaller for larger diameters; and iii) these results are more pronounced for higher noise probability. Although the general trends are clear, the results are not monotonic, and this will be discussed in the next section.

5. Discussion and Summary

The data indicate the following general trends for the concentric fiducial:

i. as the diameters are increased, the error due both to sampling and additive noise decreases;

ii. as the number of rings is increased, the error due both to sampling and additive noise decreases;

iii. as the amount of additive noise is increased, the trends of (i) and (ii) are more pronounced;

iv. as the number of rings is increased, the standard deviation of the error measurement due to additive noise is decreased; and

Although the general trends are as above, in no case are they monotonic. For the plots of error due to additive noise, there are local peaks and valleys. In one case, for noise of $P = 0.05$ in Figure 6, a valley in the plot for $d = 100$ occurs at the same r as a peak for $d = 300$, and the plots cross. Although the sample size (15 noise images) may be suspect, the standard deviations (not shown) are small and fairly consistent for all points, so small sample size is not the likely problem. An alternative explanation is some correlation between the sampling resolution and concentric pattern at certain number of rings and diameter sizes. This is similar to the explanation for the peaks in error for the diamond shape plotted in Figure 1. However, this relationship between the circle and the sampling plane is non-linear for different shifts, diameters, and number of rings, and has so far defied analysis.

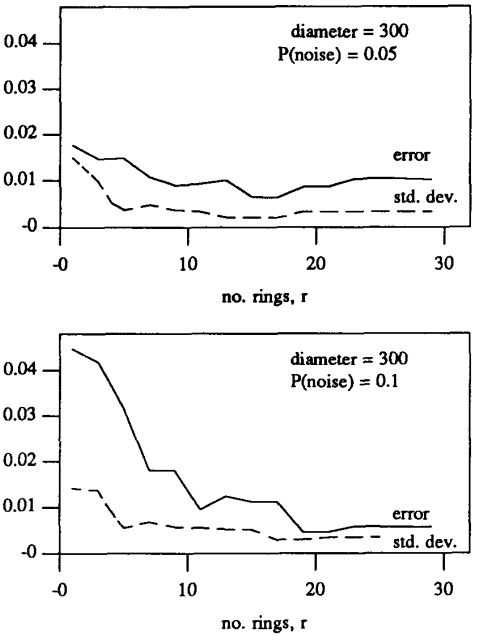

Figure 5. Plots show average and standard deviation of maximum error versus number of rings for concentric fiducials of diameter 300, with added noise of 5% on the top and 10% on the bottom.

For the plots of error due to sampling only, the general trends are observed as listed. However there are instances of more marked non-monotonicity than for the case of additive noise. Two explanations could apply here. One is that the sampling interval (0.01 pixels) was not large enough, however partial results for higher sampling resolutions (not shown here) indicated the same peaks and valleys. The other explanation is that these are due to sampling effects as discussed above. The effects would be more pronounced for this test because no averaging is performed here (in contrast to the tests for additive noise where averaging is done over many images).

As is evident from the above discussion, efforts to describe the behavior of concentric disks in a sampling plane have so far escaped mathematical explanation. The difficulty of the problem is also evident from the literature. This problem is broached in [10], but due to the difficulty of analysis, no general two-dimensional relationship was obtained. In [11], a discrete disk is analyzed, but this is done only for the more restricted case where the center is fixed on a sample point. In [8,10], it is evident that their locale, describing the region of imprecision, becomes more complex with increased region samples. The problem appears to be non-linear because the circular edges of the disks are uncorrelated with the Cartesian sampling plane. In any case this problem merits future effort..

It should be noted that, in practice, there is an upper limit on the number of rings within a certain diameter. For the centroid measurement from edges in equations (2) and (3), adjacent rings must be individually distinguishable, i.e. topology must be maintained. Therefore the practical lower limit on ring spacing is a distance such that the probability that noise will merge two rings is small. In our tests, for the different noise probabilities tested, the minimum ring spacing was five pixels.

As far as the method of ring detection, and the added computation required, this is not dealt with in this paper.

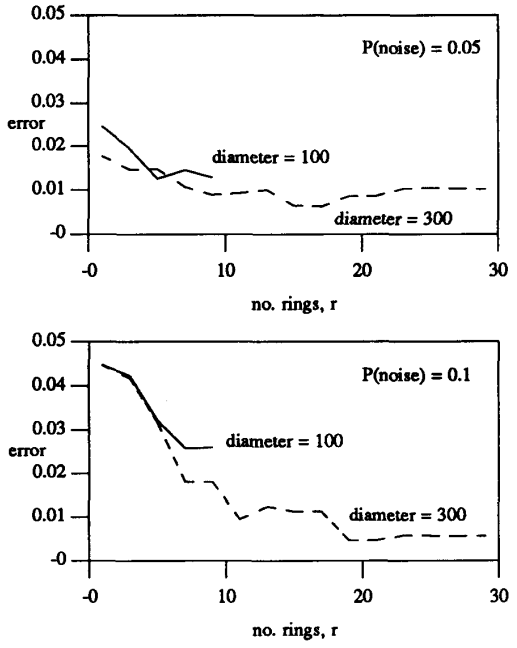

Figure 6. Plots show average of maximum error versus number of rings for concentric fiducials of diameters 100 and 300, with added noise of 5% on the top and 10% on the bottom. (Note that the plot for the diameter of 100 is only up to 9 rings. This is because pixel spacing between rings becomes too small for more rings.)

(See, for instance, reference [11] for methods of circle detection.) The straightforward method used in this paper was to find connected regions of ring boundaries, then to determine the concentric disk centroids based on these boundaries along each x,y scan line. This is not an expensive technique relative to, for instance, recursive refinement methods that might be used, but it is more computationally expensive than for the straightforward centroid calculation as in equation (1). Because of this, a decision would be made in practice whether the improved precision is worth the added complexity and computation.

In summary, it has been shown that the circular fiducial used for machine vision registration can be extended to a concentric pattern that occupies the same area, but yields better centroid estimates. A method of centroid calculation was shown that treats the fiducial with r concentric rings, as r separate but concentric disks, thus yielding a larger *effective area*. Experiments were performed to find the error in the centroid measurement due to additive noise, and due to sampling quantization. These showed that the centroid measurement was generally more accurate as the outside diameter and number of concentric rings increased. Although the benefits of this shape and method for registration have been shown by experiment, a challenging problem still remaining is to explain by analysis some non-monotonicities in the results.

Acknowledgements

We would like to thank Dave Havelock for his thorough reading of the paper and many suggestions that have been incorporated here.

REFERENCES

1. C.B. Bose, I. Amir, "Design of fiducials to facilitate inspection using machine vision", IEEE PAMI, 1990 (accepted for publication).
2. Q. Tian, M.N. Huhns, "Algorithms for subpixel registration", Computer Vision, Graphics, and Image Processing, Vol 35, No. 2, 1986, pp. 220-233.
3. H.K. Nishihara, P.A. Crossley, "Measuring photolithographic overlay accuracy and critical dimensions by correlating binarized Laplacian of Gaussian Convolutions", IEEE Trans. PAMI, Vol. PAMI-10, No. 1, Jan. 1988, pp. 17-30.
4. I.J. Cox, J.B. Kruskal, "On the congruence of noisy images to line segment models", Second International Conference on Computer Vision, Tampa, FL, Dec, 1988, pp. 252-258.
5. I.J. Cox, J.B. Kruskal, D.A. Wallach, "Predicting and estimating the accuracy of a subpixel registration algorithm", IEEE Trans. PAMI, 1990, (accepted for publication).
6. J.W. Hill, "Dimensional measurements from quantized images", in *Machine Intelligence Research Applied to Industrial Automation*, by D. Nitzan, et al., SRI 10th Report for NSF Grant DAR78-27128, 1980, pp. 75-105.
7. C.A. Berenstein, L.N. Kanal, D. Lavine, E.C. Olson, "A geometric approach to subpixel registration accuracy", Computer Vision, Graphics, and Image Processing, Vol. 40, 1987, pp. 334-336.
8. L. Dorst, A.W.M. Smeulders, "Discrete representation of straight lines", IEEE Trans. PAMI, PAMI-6, No. 4, July, 1984, pp. 450-462.
9. D.I. Havelock, H. Ziemann, "Optimal position estimation in digital image metrology", Int. Symp. Photogrammetry and Remote Sensing, Kyoto, Japan, July, 1988.
10. D.I. Havelock, "Geometric precision in noise-free digital images", IEEE Trans. PAMI, PAMI-11, No. 10, Oct. 1989, pp. 1065-1075.
11. Z. Kulpa, "On the properties of discrete circles, rings, and disks", Computer Vision, Graphics, and Image Processing, Vol. 10, 1979, pp. 348-365.
12. A. Nakamura, K. Aizawa, "Digital Circles", Computer Vision, Graphics, and Image Processing, Vol. 26, 1984, pp. 242-255.